On the acceleration in the high-β structure

Takao Kato

KEK, High Energy Accelerator Research Organization

Summary

The acceleration in the high-β structures (ACS and SC) has been examined by both estimating the space-charge effects and the rf defocusing force, and performing particle simulations. The results of the particle simulation show that the energy oscillation becomes very large, depending upon the distribution of the random errors in the accelerating field. In the SC structure within errors of 1% in the field amplitude and 1 degree in the phase, the oscillation amplitude becomes so large that the accelerated particles go beyond the longitudinal stable region, which size varies largely due to the large phase slip. It should be pointed out that there are a few kinds of mismatching sources in the SC structure: a change in rf forces due to a large phase slip, a jump both in the focusing period and in the accelerating field between the adjacent beta-cell structures. The average energy deviation of more than 2 MeV from the design output value is observed in the SC structure with random errors of 1% and 1degree in the accelerating field. In order to compensate for the energy deviation, the random errors should be suppressed sufficiently stable during the pulse width. Judging from the simulation results for the ACS structure, the beam can be accelerated stably over the wide range of errors in the accelerating parameters.

1. Introduction

There are many complex and difficult issues in the high-beta acceleration, including the space-charge effects, the rf defocusing effects and phase slip along an rf structure. Many works have been done using various analyzing tools for achieving stable acceleration in the high-β structure, ACS (Annular Coupled Structure) and SC (superconducting structure). Here, two kinds of analyses are performed: the first is to calculate the magnitude of the space-charge effects and rf defocusing effect, depending upon the type of the accelerating structures. The second is to perform many particles simulations using the most rigorous approximation for the space-charge effects and the distribution of the accelerating field.

2. The space-charge effects and the rf defocusing effects

Tune depression is usually used for representing the magnitude of the space-charge effects, defined by the ratio between the phase advance with a current and that without current. Figure 1-1 shows the calculated tune depression for a 150-mA matched beam acceleration in the ACS and SC structures at an injection beam energy of 191 MeV. It is found that the space-charge effects are stronger in the SC compared with those in the ACS, although the beam current is the same value. This is due to the fact that the extra spaces other than rf structure is longer in the SC than that in ACS.

KEY WORDS: superconducting proton linear accelerator, phase slip, rf defocusing effects, simulation

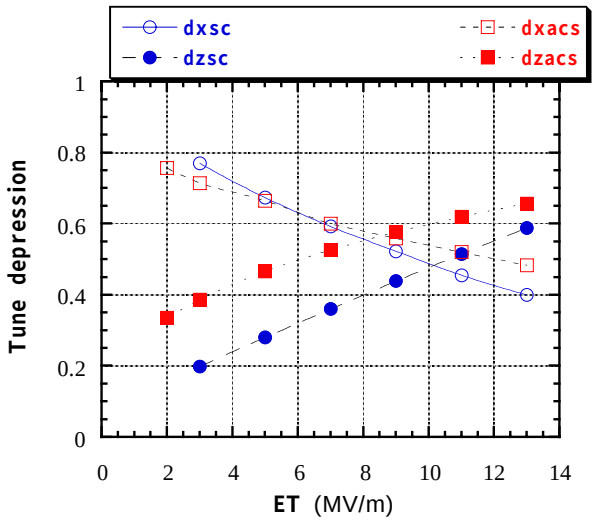

Fig. 1-1 Tune depression in the both transverse and longitudinal motion in the matched acceleration of a 150-mA beam. The transverse zero-current phase advance of 90 degrees is assumed. The ACS structure of Type-5 in Table 1 and the updated JAERI SC-design are used in the calculation.

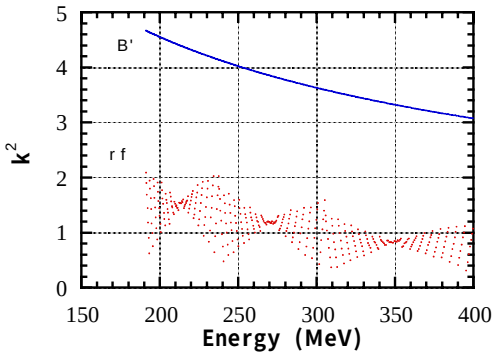

Fig. 1-2 The external force and the rf defocusing force along the SC 3-beta-cell linac. The rf defocusing force of each cell is multiplied by the number of cells in a tank in order to compare the external force.

The rf defocusing effects are rather large in spite of the high-energy acceleration, since the high-β structure contains many numbers of rf gaps of a high accelerating field. In addition, the rf defocusing force varies largely due to the phase slip in the SC structure. The focusing forces are written as:

external focusing force:

$$k_q^2 = \frac{q}{mc^2}\frac{cB'}{\beta\gamma},$$

rf defocusing force:

$$k_{rf}^2 = -\frac{q}{mc^2}\frac{\pi E_0 T \sin\varphi}{\lambda\beta^3\gamma^3},$$

where m is the proton mass, c the light velocity, q the unit charge, βγ the usual kinematic parameters, B' the magnetic field gradient, E_0 the accelerating field, T the transit time factor, ϕ the rf phase and λ the wave length. Figure 1-2 shows the calculated focusing forces in the SC proton linac (190 – 400 MeV, using three kinds of beta-cell structures) designed by the JAERI group (ref.1). There are two kinds of periods in the rf defocusing force: The first is a change of more than three times in a tank due to the phase slip. The second period corresponds to the number of beta-cell structures in the linac, since the range of the phase slip in a structure is determined primarily by the difference between the beta of the particle and that of the cell. These facts imply that the transverse focusing force changes with two kinds of periods mentioned above, resulting some local mismatching along the linac. There is also modulation of longitudinal focusing force in the SC.

3. Particle simulation

The simulation was performed using the modified code for calculating a SC proton linac structure, CCLINSAC, which was at first written as LINSAC for calculating the beam behaviour in DTL. The space-

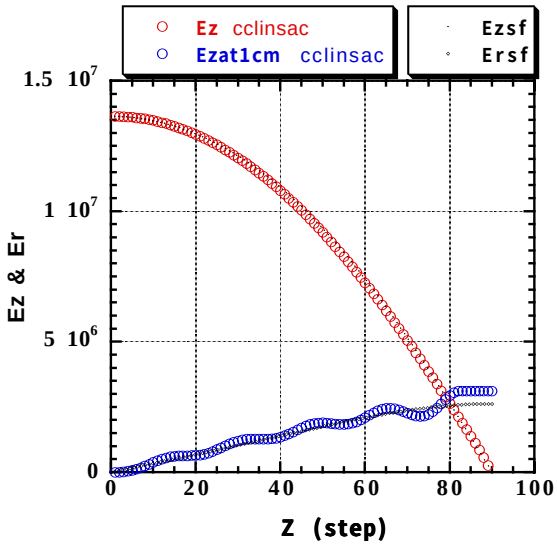

Fig. 2 Calculated field distributions in a cell. The circles indicate the results of CCLINSAC, the dots by SUPERFISH.

charge effects are taken into account by particle-particle (p-p) method, including modification for suppressing overestimation when the two particles become very close. The accelerating field in the code is approximately calculated by using polynomial formula. The radial fields are calculated using general electromagnetic formula. Figure 2 shows the comparison between two field distributions in a gap, calculated with SUPERIFSH and the CCLINSAC code, both for the accelerating field (E_z) and the radial field (E_r). The number of macro-particles used in the simulation is 3200. A 150-mA beam is used.

In order to estimate the structure difference between SC-type and ACS-type, the same code, CCLINSAC, is used for both SC and ACS simulations. Because of the code limitation, there is a drift space ($\beta\lambda/2$) between the two adjacent ACS-tanks of seven cells, corresponding two tanks in a cooling tank in the SC structure. The geometry of the focusing section is the same for both structures. Thus, the ACS tanks consists 14 cells and a drift of a unit cell. Therefore, the simulation was performed not for comparing the SC and normal conducting structures, but for comparing the effects of the constitution of two types of structures. Here, according to the widely known design method, the cell length in the SC structure keeps constant over some numbers of the tanks, resulting a large phase slip in the tank. Therefore, the main differences between the SC and the ACS are; the length of focusing period, amplitude of the accelerating field and the change of the stable phase.

.

3.1 Design of linac

Five kinds of linac design (four SC-type and one ACS-type) are summarized in Table 1. Here, the simulation results for the Type-3 and Type-5 are presented. The rf stable phase varies from -66 to -13 ° . The transverse focusing was performed with doublet system between two tanks; two quadrupole magnets of 0.2 m in length and a 0.2-m space between them. The length between the tank and the magnet is 0.93 m for SC and 0.05m for ACS. The length between two tanks, that are in the cooling tank, is about 0.5 m for SC and a cell length for ACS.

Table 1 Main parameters of the five kinds of linac designs.

	Type-1	Type-2	Type-3	Type-4	Type-5
No of β-cell	2	3	4	5	ACS type
Number of tank	61	48	34	34	46
Number of cell	6	7	9	9	14
Total length	128.9	104.2	80.1	80.2	109.2
Structure length	35.8	32.9	29.9	30.0	68.2
E_0 (MV/m)	9.2, 11.1	9 - 12	8.9 – 12.6	8.9 – 11.9	4.29

3.2 Design of ACS linac

The ACS-type (Type-5) was designed for comparison with the SC-Type. The ACS tank consists of two unit tank of seven cells and a drift space of a half beta-lamda between them. The magnitude of the phase slip is small, since the optimum cell length is used for each tank.

3.3 Emittances of the injected beam

The output-emittance magnitude of the accelerated beam through the DTL and the SDTL of the joint project was used for the injection beam into the SC and ACS; normalized rms transverse emittance is 0.24 π-mm-mrad and rms longitudinal one is 0.460 π -MeV-deg.

3.4 Results of SC structure

The simulation results for the SC structure (Type-3) are presented. The focusing strength at the injection was determined so that the zero-current transverse phase advance was 90 degrees. The magnetic gradient held constant through the linac. Figure 3 shows the rms (x,y,z) beam sizes along the SC structure.

Figures 4 – 9 show the output emittances.

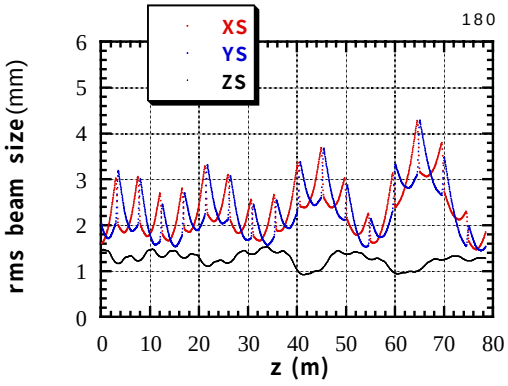

Fig. 3 SC (no error): beam sizes.

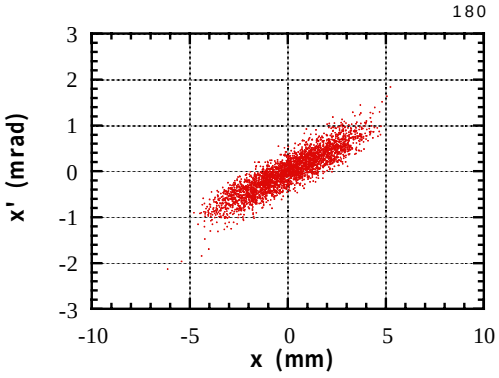

Fig. 4 SC (no error): x-x'

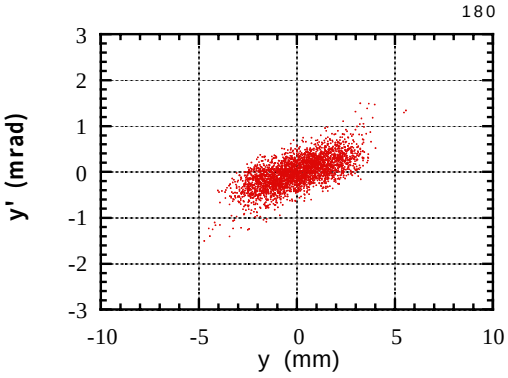

Fig. 5 SC (no error): y-y'

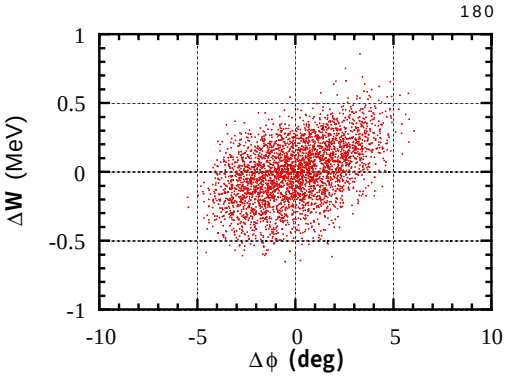

Fig. 6 SC (no error): Δϕ-Δw

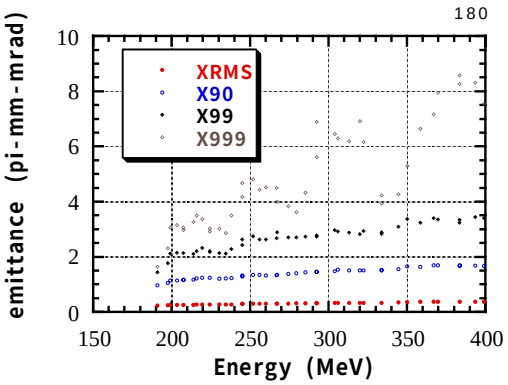

Fig. 7 SC (no error): x-x' emittance variation.

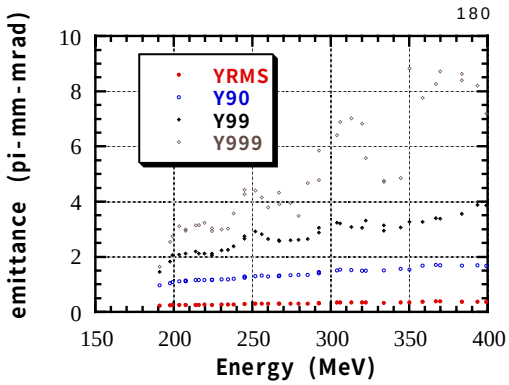

Fig.8 SC (no error): y-y' emittance variation.

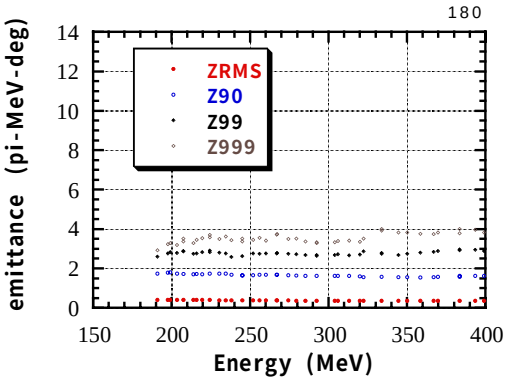

Fig. 9 SC (no error): Δϕ-Δw emittance variation.

Judging from the simulation results, the stable acceleration can be achieved if there were no errors in the SC accelerating parameters. It can be seen from the figures that there are some mismatch effects due to the change in the cell-beta structure, at energies of 224, 267 and 320 MeV, especially in the transverse emittances. There is possibility that some injection errors are increased by the transitions due to the change in cell-beta. Generally speaking, the accelerating parameters vary largely at the cell-beta transition in order to increase accelerating efficiency or achieve stable acceleration. As a result, there are transitions in both the transverse and longitudinal motion. The accelerating period usually changes since the cell length changes.

3.5 Results of ACS structure

The simulation results for the ACS structure (Type-5) are presented. The focusing strength at the injection was determined so that the zero-current transverse phase advance was 90 degrees. The magnetic gradient held constant through the linac. Figure 10 shows the rms (x,y,z) beam sizes along the ACS structure. Figures 11-16 show the output emittances.

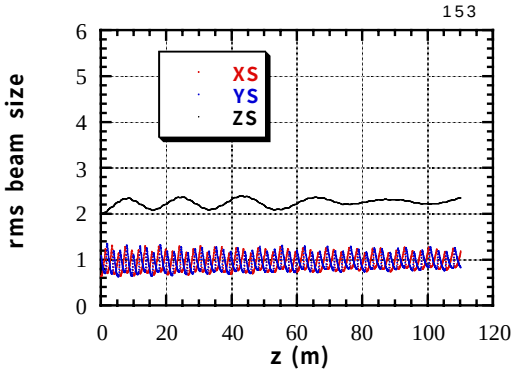

Fig.10 ACS (no error): beam sizes.

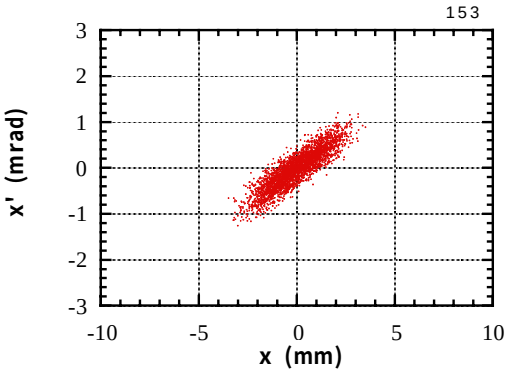

Fig.11 ACS (no error): x-x'

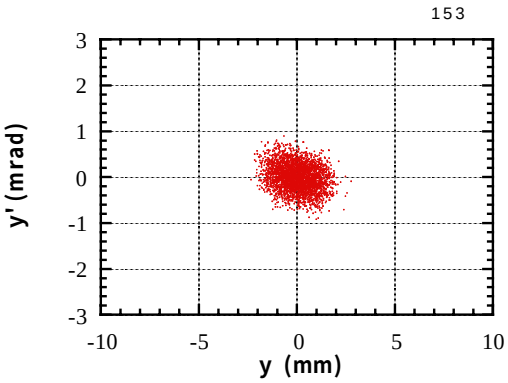

Fig.12 ACS (no error): y-y'

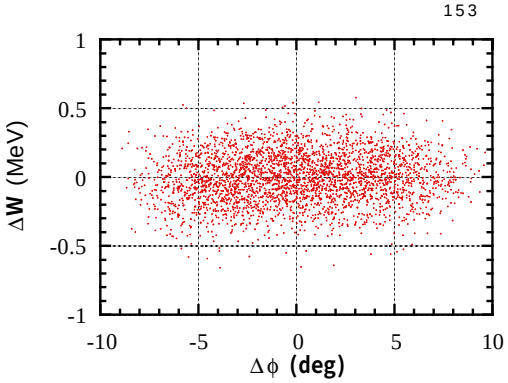

Fig.13 ACS (no error): Δϕ-Δw

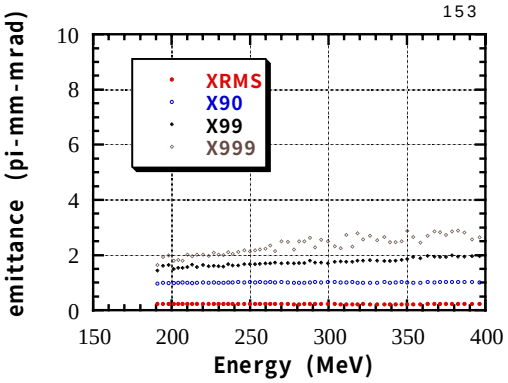

Fig.14 ACS (no error): x-x' emittance variation.

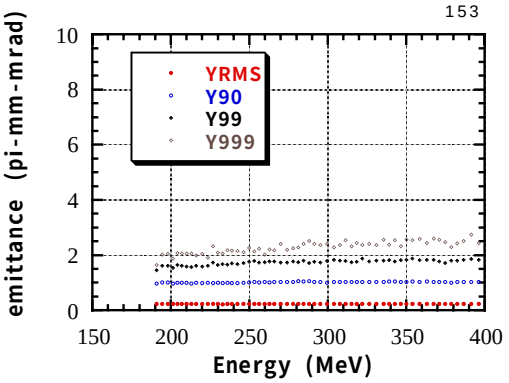

Fig.15 ACS (no error): y-y' emittance variation.

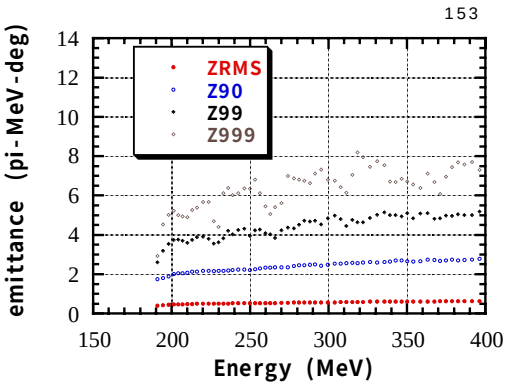

Fig.16 ACS (no error): Δϕ-Δw emittance variation.

A stable acceleration is possible if there were no errors in the ACS accelerating parameters. As compared with the SC results, the increase in the longitudinal emittance is noticeable. There are two reasons for the increase: the first is the relatively week focusing strength compared with the SC acceleration, the second is larger mismatch at the longitudinal injection, judging from the variation of the longitudinal beam size just after the injection.

3.6 Results of the error simulation

3.6.1 Large transverse mismatch in the ACS

There is some possibility that the oscillation in the transverse motion in the SC structure (Fig.3) is due to the mismatch in the injection. In order to confirm the assumption, a simulation with a large transverse mismatch at the injection was performed. Figure 17 shows the variation of rms beam sizes along the ACS structure when the one of the injection twiss-parameter (beta-x) was increased by a factor of 2.5.

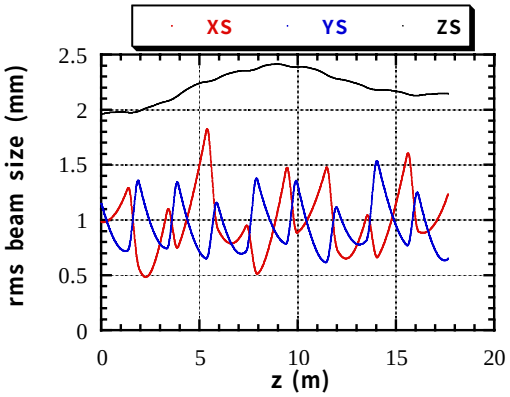

The oscillation of the rms x-beam size can be seen in the Fig. 17. However, the behaviour is different from that in the Fig. 3. Since the oscillation in the transverse motion (Fig. 3) was vanished with a test calculation in which the rf defocusing term was set zero, the oscillation is due to the rf defocusing effects, combined with the phase slip, although the initial mismatch in creases the effects. There are some possibilities that the oscillation will disappear after tuning of the accelerating parameters. However, since the coupling between the transverse and longitudinal motion is not large, here, we think the simulation mentioned in Fig. 3 as the starting run for the SC structure.

3.6.2 Results of simulations with errors in the accelerating field amplitude and phase

The simulation results with the random errors in the accelerating field amplitude and phase are presented. The errors for each cell and each tank are considered. The notation of the errors is as follows:

E31: each cell field error of 3%, each tank field error of 1%,

P21: each cell phase error of 2 degrees, each tank phase error of 1degree.

The errors are generated uniformly. In the next section, we will refer to the dependence of the distribution of the errors along the structure. Here, the simulation results, which seem to be largely affected by the error distribution of E21P11, are presented, since we are now studying the feasibility of the structure.

Tables 2 and 3 list the output emittances for the ACS and SC simulations, respectively.

Table 2 Summary of ACS emittance (π cm-mrad, π MeV-deg)

	X			Y			Z			
	rms	90%	100%	rms	90%	100%	rms	90%	100%	
INPUT	.0229	.0976	.1759	.0232	.0979	.1764	.4508	1.921	3.507	
No error	.0231	.1021	.3257	.0230	.1031	.2690	.7069	3.057	9.407	run153
E11P11	.0230	.1003	.5710	.0228	.1043	.4996	.7469	3.203	11.61	
E21P11	.0231	.1053	.3642	.0234	.1081	.3414	.7927	3.537	11.69	run215
E21P11	.0230	.1050	.3431	.0225	.101	.4190	.7613	3.234	10.55	run193
E11P33	.0229	.1038	.3921	.0230	.1030	.4541	.7479	3.180	11.77	
E31P33	.0230	.1014	.5343	.0234	.1041	.3016	.7346	3.195	10.05	

Table 3 Summary of SC emittance (π cm-mrad, π MeV-deg)

	X			Y			Z			
	rms	90%	100%	rms	90%	100%	rms	90%	100%	
INPUT	.0229	.0976	.1759	.0232	.0979	.1764	.4508	1.921	3.507	
No error	.0386	.1684	.9896	.0386	.1685	.8604	.4099	1.794	6.196	
E11P11	.0504	.2368	1.419	.0534	.2518	1.517	.9320	4.203	20.75	run182
E21P11	.0557	.2618	2.628	.0596	.2902	1.687	1.186	5.176	31.01	run181
E11P11	.0361	.1665	.6098	.0376	.1754	.6341	.5102	2.282	10.42	run203

As for the ACS acceleration, there is no large increase in the emittances within the errors in Table 2.

As for the SC acceleration, the error tolerance for the longitudinal motion seems very small. Even in the errors within 1degrre and 1 % in the accelerating field, the output beam emittances greatly increase, depending upon the error distribution. Figures 18 - 31 show the results for SC (left side) and ACS (right side) with an error of E21P11. The results presented are the worst cases among sixty runs of simulation for each structure.

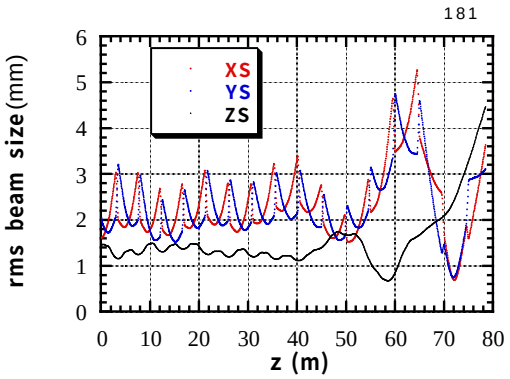

Fig. 18 SC: error E21P11

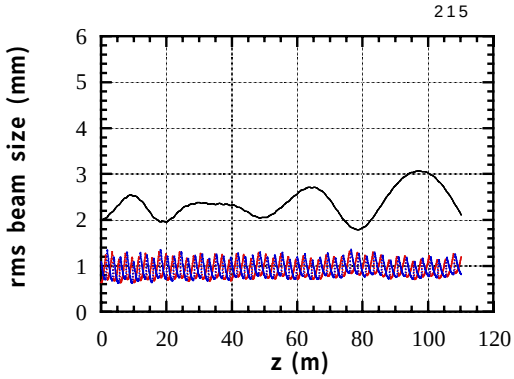

Fig. 19 ACS: error E21P11

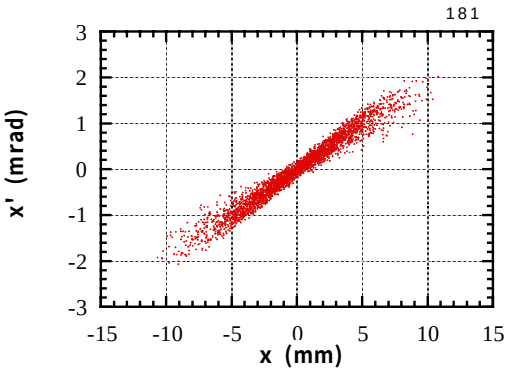

Fig. 20 SC: error E21P11

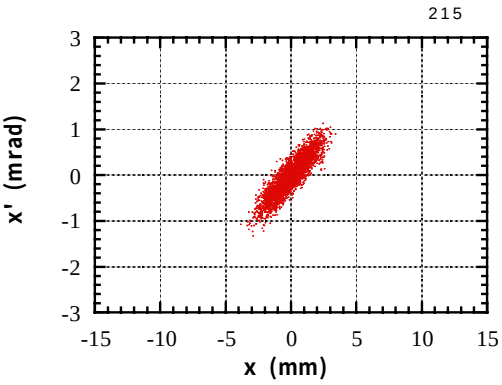

Fig. 21 ACS: error E21P11

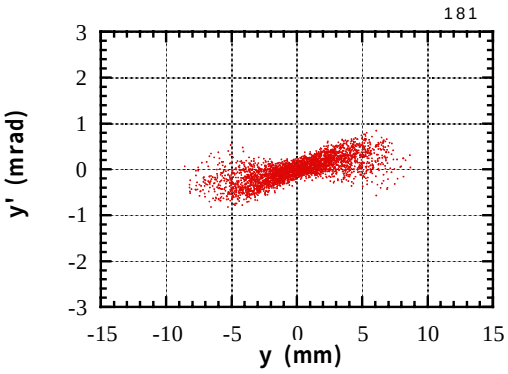

Fig. 22 SC: error E21P11

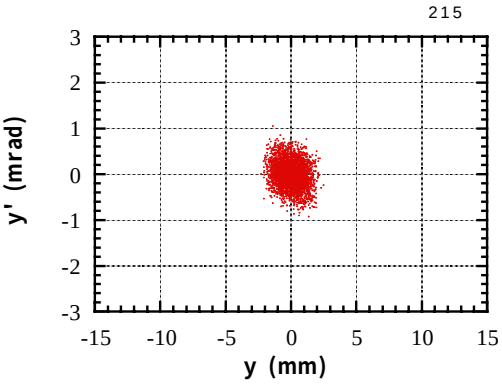

Fig. 23 ACS: error E21P11

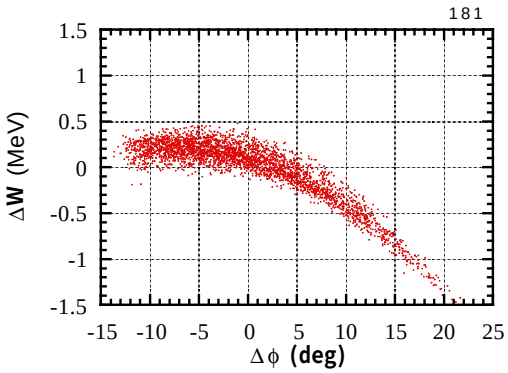

Fig. 24 SC: error E21P11

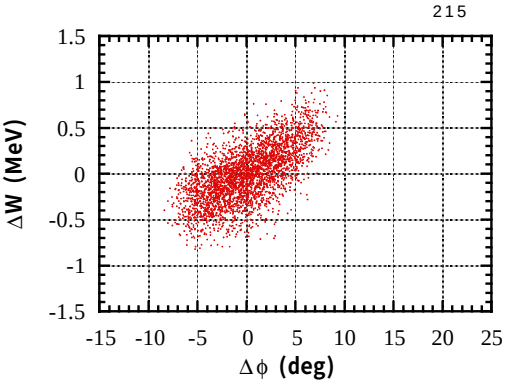

Fig. 25 ACS: error E21P11

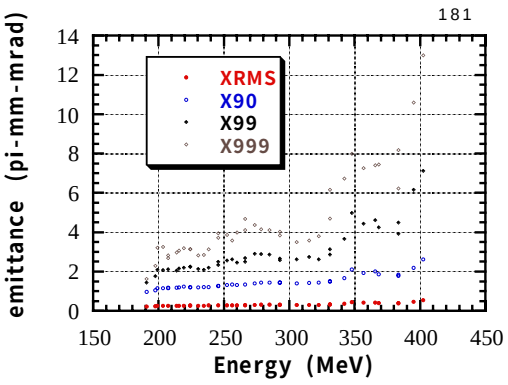

Fig. 26 SC: error E21P11

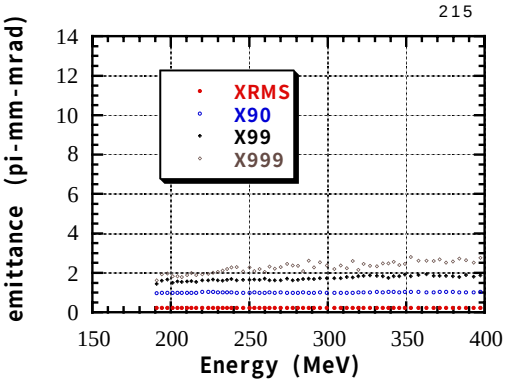

Fig. 27 ACS: error E21P11

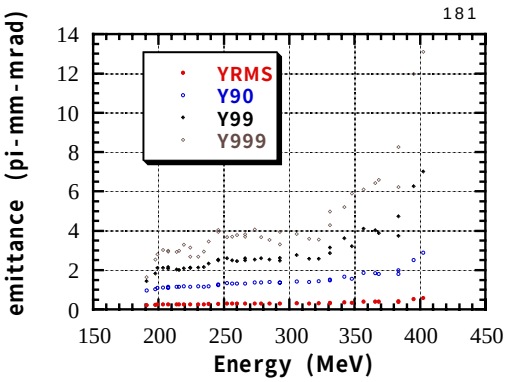

Fig. 28 SC: error E21P11

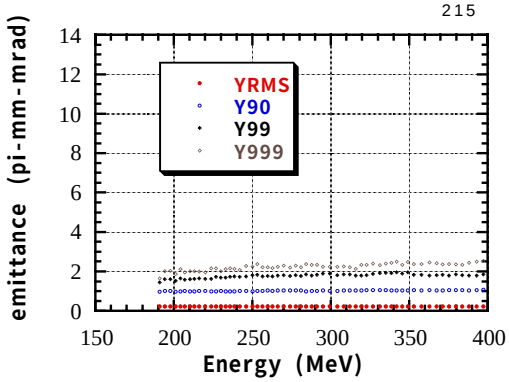

Fig. 29 ACS: error E21P11

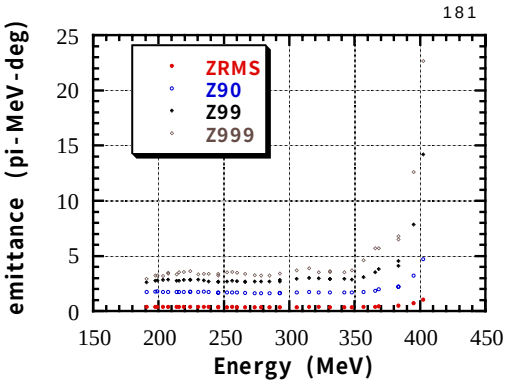

Fig. 30 SC: error E21P11

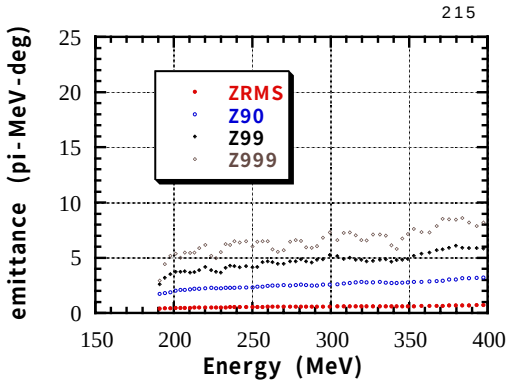

Fig. 31 ACS: error E21P11

3.6.3 Dependence upon the error distribution

The simulation results depend upon the distribution of the errors along the structure. Then, sixty runs of random-error simulation for both SC and ACS were performed with the same starting value for the random-error distribution of E11P11. Figure 32 shows the deviation of the output energy from the design value versus the maximum energy-oscillation amplitude in the structure. It was found that four runs among sixty were unstable in the SC structure. The energy oscillations along the structures with/without errors (E21P11) in the accelerating field are shown (Figs. 33 - 36).

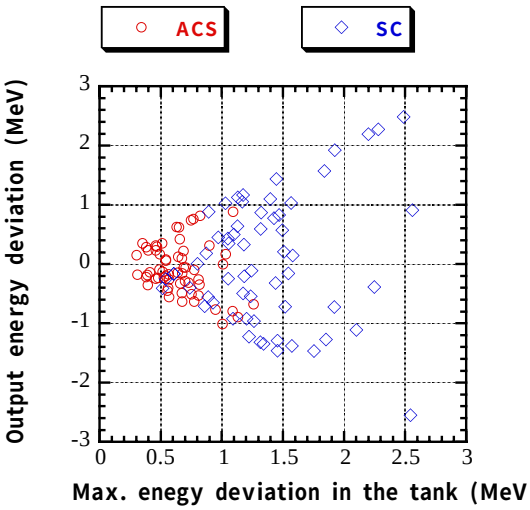

Fig. 32 Deviation of the output energy from the design value versus the maximum energy-oscillation amplitude in the structure for sixty random-error simulation. The error of E11P11（1 ° 1%）is assumed.

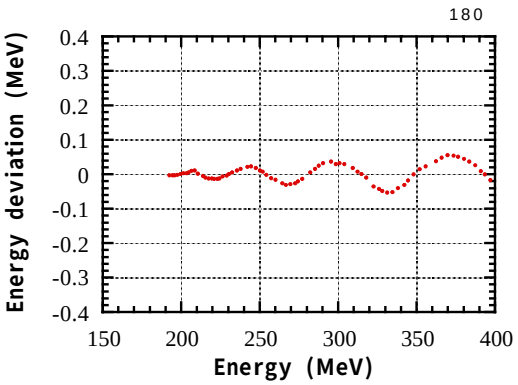

Fig. 33 SC: energy oscillation (no error)

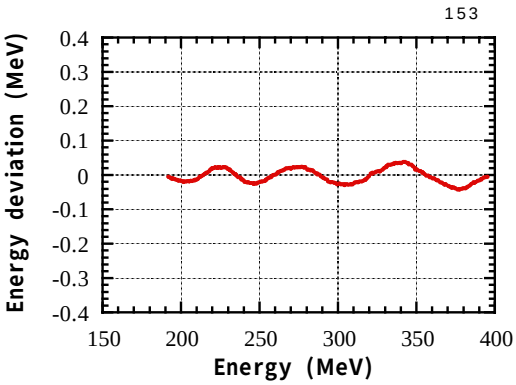

Fig. 34 ACS: energy oscillation (no error)

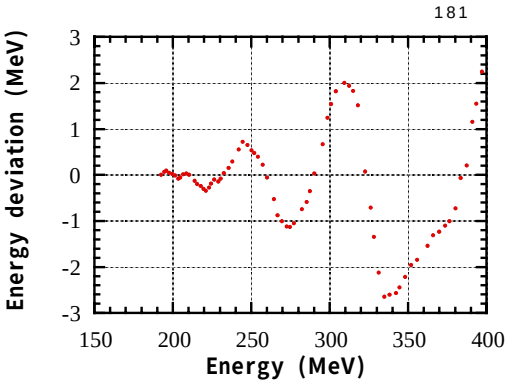

Fig. 35 SC: energy oscillation (error E21P11)

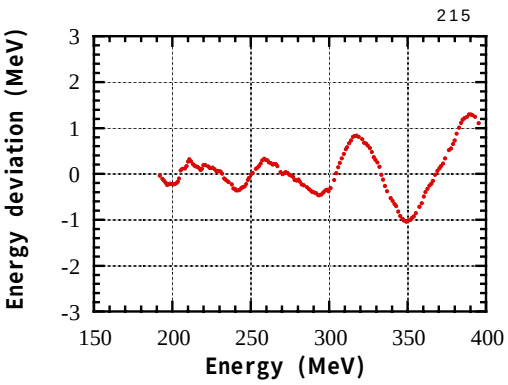

Fig. 36 ACS: energy oscillation (error E21P11)

4. Discussion

In the design of the SC proton linac, the number of cell-beta is usually reduced in order to achieve the reduction of cost. Then, the amount of the phase slip in the tank increases, resulting bad effects on the beam acceleration. There are transitions between the different cell-beta structures. Here, the accelerating parameters,

such as the field amplitude, rf phase and focusing period, usually change largely. It is sometimes observed in the proton linac that the longitudinal oscillation, excited by some kinds of mismatch and errors along the structure, is largely amplified. If the local longitudinal acceptance at the some region along the structure becomes small, a part of the beam will go beyond the stable region. This is the reason for the bad longitudinal output emittance even in the errors of 1 degree and 1 % of the accelerating field. We have observed four such cases out of sixty random-error SC simulation. In the pulsed SC proton linac, there are many reasons, which cause the random errors in the accelerating field: Lorentz detuning effects, micro-phonics vibration, beam induced field and the rather long transient time constant. Thus, many types of random error distribution will be expected during the beam pulse duration. The amplitude of the energy oscillation is proportional to the square root of the accelerating field. Then, the deviation of the output energy from the design value increases as the accelerating field increases. Therefore, even within the errors of 1 degree and 1% in the accelerating field, the deviation of the output energy becomes too large for compensation so long as the error amplitude and distribution along the structure change during the pulse duration.

Acknowledgments

The author wishes to express his gratitude to Y. Yamazaki, K. Hasegawa, M. Ikegami and the members of the beam dynamics group of the Joint Project for valuable discussions.

Reference

1. K. Mukugi, JAERI-PAL note, PA01-001-R, 4/6/2001.